



This is a repository copy of *Pyro processing cement kiln bypass dust : enhancing clinker phase formation*.

White Rose Research Online URL for this paper:
<https://eprints.whiterose.ac.uk/165081/>

Version: Accepted Version

Article:

Hanein, T. orcid.org/0000-0002-3009-703X, Hayashi, Y., Utton, C. et al. (4 more authors) (2020) *Pyro processing cement kiln bypass dust : enhancing clinker phase formation*. *Construction and Building Materials*, 259. 120420. ISSN 0950-0618

<https://doi.org/10.1016/j.conbuildmat.2020.120420>

Article available under the terms of the CC-BY-NC-ND licence
(<https://creativecommons.org/licenses/by-nc-nd/4.0/>).

Reuse

This article is distributed under the terms of the Creative Commons Attribution-NonCommercial-NoDerivs (CC BY-NC-ND) licence. This licence only allows you to download this work and share it with others as long as you credit the authors, but you can't change the article in any way or use it commercially. More information and the full terms of the licence here: <https://creativecommons.org/licenses/>

Takedown

If you consider content in White Rose Research Online to be in breach of UK law, please notify us by emailing eprints@whiterose.ac.uk including the URL of the record and the reason for the withdrawal request.



eprints@whiterose.ac.uk
<https://eprints.whiterose.ac.uk/>

1 Pyro processing cement kiln bypass dust: enhancing clinker phase 2 formation

3 Theodore Hanein^{a*}, Yuki Hayashi^a, Claire Utton^a, Magnus Nyberg^b, Juan-Carlos Martinez^b,
4 Nestor-Isaias Quintero-Mora^c, and Hajime Kinoshita^{a*}

5 ^a*Department of Materials Science & Engineering, University of Sheffield, Sheffield, S1 3JD, UK*

6 ^b*CEMEX Asia Research AG, Römerstrasse 13, 2555 Brugg, Switzerland*

7 ^c*CEMEX Operaciones Mexico, Constitution 444 pte. Monterrey, Mexico*

8 **Corresponding authors: t.hanein@sheffield.ac.uk & h.kinoshita@sheffield.ac.uk*

9 Abstract

10 The valorisation of cement kiln bypass dust (CBPD) is explored for sustainable production of
11 cementitious clinker phases. CBPD can replace the calcareous component in cement
12 manufacture and allow for a reduction in CO₂ emissions as the calcium component in CBPD is
13 mostly decarbonised. CBPD was heated with/out the addition of alumina or silica at
14 temperatures of 900 – 1100°C to produce clinker phases. Belite and mayenite formed at
15 temperatures as low as 900°C, while alite formation was achieved at 1200°C, which is
16 significantly lower than is conventional (~1450°C). Alite is thermodynamically stable only
17 above 1250°C; thus, the reduced temperature is potentially owing to the presence of chloride
18 found in the CBPD (as KCl) which was also eventually simultaneously removed through pyro
19 processing at 1100 – 1200°C. The investigation also confirmed that the formation of belite is
20 enhanced in the presence of molten KCl.

21 **Keywords:** Cement kiln bypass dust; cement manufacture; clinker; pyro processing; waste
22 valorisation; low-carbon clinker

23

24 **1. Introduction and background**

25 The cement industry is generating and emitting significant quantities of carbon dioxide (CO₂)
26 that amounts to approx. 8% of global man-made emissions [1]. In Portland cement (PC)
27 manufacture, approximately 90 % of the CO₂ emissions are direct emissions from the burning
28 of fossil fuels (~30%) and the decomposition of calcium carbonate (~60%), mainly from
29 limestone, with the remaining ~10% being indirect emissions such as electricity consumption
30 [2]. The burning of the fuels is necessary to reach a temperature of approximately 1450°C, for
31 clinkering.

32 Modern manufacture of PC utilises the preheater rotary kiln configuration. To avoid damage
33 in subsequent concrete, cement clinker is designed to meet the low-alkali and chlorine
34 specifications; thus, a bypass is used to extract the dust containing air which includes alkali,
35 sulphates, and chlorides that originated from the kiln raw meal or fuel. The bypass also helps
36 break the volatilisation cycle within the process and avoid kiln operational problems. The
37 bypass is positioned between the kiln inlet and the preheater to extract dust-containing air,
38 where temperatures exceed 900°C; thus, the calcareous component in the collected dust will
39 be mostly decarbonised. The removed solids/dust is called cement kiln bypass dust (CBPD),
40 and the amount of this dust produced is approximately 2% of clinker production by weight.
41 Global cement production of 4.1 billion tonnes in 2017 [3] equates to a substantial amount of
42 bypass dust being generated. It should be noted that not all kilns are equipped with a bypass
43 and kilns with a bypass system are more frequent in Europe, and to some extent the USA,
44 than in other regions. CBPD is often classified as cement kiln dust (CKD); but, the two are not

45 the same and should be differentiated. CBPD is collected from the bypass only while CKD can
46 be collected from the flue gas leaving the preheater tower at lower temperatures and is
47 produced in larger quantities (15 – 20 times) than CBPD. CKD will contain calcium carbonate
48 and less chloride and unlike CBPD, CKD is generally recycled during cement manufacture
49 either as raw meal or blended with the final cement while CBPD is not.

50 CBPD is usually unexploited and landfilled at a monetary and environmental cost. The
51 recycling of CBPD is interesting due to its the negative effects on human health and
52 ecotoxicity [4, 5]. Research on the valorisation of CBPD has focused on using it as an additive
53 to cement [6], for backfilling excavations [7], for sand and soil stabilization [8, 9], to activate
54 slags in cement blends [10], for the manufacture of vitrified sewer pipes [11]; or, thermally
55 treated along with other material to produce glass/ceramic for sustainable disposal [12] or
56 pozzolanic cementitious material [13]. The production of cement clinker from CBPD has not
57 been previously studied and will be explored in this work.

58 CBPD is mainly composed of calcium oxide (CaO), which is the key component in traditional
59 cement clinker. Differing from the limestone used for the conventional clinker production,
60 the calcium component in the CBPD is already in the de-carbonised form; thus, producing
61 cement from this material can allow for the reduction in the raw-material derived carbon
62 emissions. Additionally, CBPD contains salts (such as KCl) that will melt at temperatures
63 approaching clinkering conditions. These salts can act as a flux to improve the extent of
64 reactions [14] and can be used to reduce the temperature required for cement manufacture
65 [15-17]; thus, enabling a reduction in fuel-derived CO₂ emissions.

66 Cement production is on the rise and with it, the production of CBPD. Further utilisation of
67 CBPD is therefore advantageous in order to minimise its negative influence over the
68 environment and the cost of landfilling. The aim of the title study is to explore the pyro
69 processing of CBPD with/out additives for potential manufacture of low-carbon cement
70 clinker or supplementary cementitious material, and at reduced temperatures than
71 conventional; thus, extending the reusability of the by-product in the conventional cement
72 production process and promoting green and circular solutions in the cement industry.

73 **2. Objectives**

74 This work seeks to assess the valorisation of CBPD through the pyro processing/calcination of
75 CBPD with/out the addition of alumina and silica in order to understand the influence of the
76 intrinsic minor components on clinkering. Components within the CBPD can enhance the
77 formation of cementitious clinker phases at a lower temperature than is conventional, by
78 acting as a flux/mineraliser or through entropy stabilisation due to ionic substitution in clinker
79 phases. The thermal treatment will also be used to burn off the undesirable salts within the
80 mix. CBPD and blends with SiO_2 and/or Al_2O_3 are heated at 900 – 1200°C and the phases
81 formed are presented. Reagent grade Al_2O_3 and SiO_2 , are used as surrogates for clays to
82 demonstrate separately the formation of silicate and aluminate phases. For application,
83 aluminosilicate sources will need to be added to the raw-mix before firing in order to avoid
84 the persistence of free CaO. To elucidate the role of minor components/impurities, the minor
85 components found in CBPD and in similar quantities are blended individually with reagent
86 grade raw materials to produce a “simplified CBPD” before firing.

87 3. Materials and methods

88 3.1. Clinker phase notation

89 The cement oxide notation used in this work is: C = CaO, S = SiO₂, A = Al₂O₃, and F = Fe₂O₃.
 90 Major clinker phases are presented as alite (C₃S), belite (C₂S), ferrite, (C₂(A_xF_{1-x})) where 0 < x
 91 < 1), and mayenite (C₁₂A₇); although these phases may have incorporated other minor
 92 elements, this was not examined in the course of this work. All belite reported in this work
 93 was detected as the larnite (beta) polymorph and no other polymorphs of belite were
 94 detected.

95 3.2. Materials

96 Cement kiln bypass dust (CBPD) used in the title study was provided by CEMEX Asia Research
 97 AG and originated from an EU cement plant. To remove the moisture content in the powder,
 98 the CBPD was dried overnight in an oven at ~80°C prior to the detailed characterisation and
 99 successive experimental work. The following reagent grade materials: Al₂O₃, CaCO₃, Fe₂O₃,
 100 MgO, CaSO₄.2H₂O, SiO₂ (quartz), and KCl were also used in the present study as additives.
 101 Details on the reagent grade chemicals are provided in Table 1.

102 *Table 1: Details of the reagent grade chemicals used in this work.*

	SiO ₂	Al ₂ O ₃	CaCO ₃	Fe ₂ O ₃	MgO	CaSO ₄ .2H ₂ O	KCl
Purity	≥95%	99%	99%	≥95%	98%	≥98%	≥99%
Supplier	Sigma- Aldrich	Acros Organics	Acros Organics	Fisher Scientific	Acros Organics	Acros Organics	Sigma- Aldrich
Code	83340- 1kg	21570010	450680010	I/1013/60	205150025	225275000	P9333- 500G

104 **3.3. Methods used to characterise CBPD and pyro processed samples**

105 X-ray diffraction (XRD) was used throughout the present investigation to identify the phases
106 in the raw CBPD and pyro processed samples. A Bruker D2 PHASER was used on powdered
107 materials with a Cu-K α radiation source operating at 30kV and 10mA. For the measurements,
108 the 1 mm primary divergence slit was used with the 3 mm air scatter screen module. X-ray
109 patterns were collected in the range of 5 – 70° 2 θ at 0.02° increments and 0.5 s per step. The
110 lower and upper discriminator settings were set to 0.11 V and 0.25 V respectively and samples
111 were rotated at 15 rpm. The collected diffraction patterns were assessed using the
112 DIFFRAC.SUITE EVA software furnished with the PDF-4 2019 database.

113 X-Ray Fluorescence (XRF) was used to determine chemical composition of the dried CBPD.
114 The measurement was conducted using a PANalytical Zetium instrument and the PANalytical
115 Omnia package was used to determine the elemental concentrations in weight %. The 40
116 mm beads were prepared for the measurements using a Claisse LeNeo Fluxer by mixing 1 g
117 of sample with 10 g of lithium tetraborate salt (with 0.5% LiI). The mixture was fused through
118 heating in 5 steps before being poured and cooled: 1) 4 min at 1065°C, 2) 3 min at 1065°C
119 rocking at 10 rpm and an angle of 15°, 3) 6 min at 1065°C rocking at 30 rpm and an angle of
120 40°, 4) 1 min at 1000°C, and 5) 4 min at 1000°C rocking at 25 rpm and an angle of 45°.

121 Inductively coupled plasma – optical emission spectrometry (ICP-OES) was also used to
122 support the compositional analysis of the CBPD. A Spectro-Ciros-Vision optical emission
123 spectrometer was used for the measurement. Two or more emission lines were used to
124 determine the elements and eliminating the risk of spectral overlap interferences. Calibration

125 was conducted using multi-element standards of known concentrations from certified stock
126 solutions. Samples were prepared by dissolving 0.125 g of CBPD in 5 mL of concentrated HNO₃
127 in a glass tube, placed into the heating block and the temperature gradually raised to 150°C
128 and maintained for 15 minutes. After cooling, the solution was diluted to 50 mL. A 20-fold
129 dilution was then measured. Samples were also prepared using a combination of aqua regia
130 and HF, or a combination of HNO₃ and HF. Either 0.0625 g or 0.03125 g of CBPD was mixed
131 with 12 mL of aqua regia or 5 mL of HNO₃ in a PTFE tube, heated at 150°C for 30 minutes; 1
132 mL of HF was then carefully added, and the samples were allowed to reflux for 10 minutes.
133 Then, 1 mL HNO₃ or 2 mL aqua regia as well as 1 mL HF was added and left for a further 10
134 minutes. Solutions were immediately transferred to a larger tube to make up to 50 mL with
135 1 % nitric acid. Samples were shaken and analysis of 20-fold and 600-fold dilutions with 1 %
136 nitric acid was immediately carried out; the 600-fold dilution was used to analyse the bulk
137 elements and the 20-fold dilution was used to measure minor elements.

138 Simultaneous thermal analyses through thermogravimetric analysis (TGA) and differential
139 scanning calorimetry (DSC) were also conducted on the dried CBPD in order to explore its
140 behaviour at various temperatures. Measurements were made on approximately 30 mg of
141 sample in an alumina pan using a TA Instruments SDT Q600 operating from 20 – 1400°C with
142 a heating rate of 10 °C/min under 100 mL/min flowing nitrogen gas.

143 **3.4. Pyro processing CBPD**

144 Pyro processing of CBPD was first investigated without any additives, i.e., the CBPD was
145 subjected to high temperatures. The CBPD samples were prepared in the form of powder (3

146 g per sample) and pellet (1.5 g × 2 pellets per sample). Pellets were made using a hydraulic
147 press with a mould diameter of 2 cm and applying pressure of 64 MPa for one minute. The
148 pellet-pressing from powder was conducted without the addition of any liquid. The samples
149 were placed in 30 mL alumina crucibles and introduced into a muffle furnace preheated in air
150 at three different temperatures: 900°C, 1100°C, or 1200°C. The minimum heating
151 temperature of 900°C was selected to allow for the melting of the potassium chloride present
152 in the CBPD and with an aim of providing a flux. Three heating times studied were: 30, 60, and
153 120 minutes both for the powder and pressed samples. Considering the drop in the furnace
154 temperature by approximately 50°C when introducing the samples, the initial 10 minutes
155 were discarded from the heating time (30, 60, or 120 mins); this allowed for the furnace
156 temperature to return to the temperature targeted. After the designated heating times,
157 samples were directly removed from the furnace still at the target temperatures and cooled
158 in air at ambient conditions. Samples were then weighed and ground using a mortar and a
159 pestle for further analyses.

160 **3.5. Interaction of CBPD with additives**

161 Experiments were conducted to test the formation of targeted cement clinker phases (alite,
162 belite, and mayenite) with the addition of SiO₂ and Al₂O₃. These experiments were conducted
163 also to assess the effectiveness of salt content as a flux to obtain enhanced reaction to clinker
164 phases at reduced temperatures. The amount of SiO₂, Al₂O₃ and CBPD was calculated to
165 generate a total sample weight of 3 g based on the XRF data (shown in the result section), if
166 all CaO content would react to form the desired target phase.

167 The processing temperatures and the composition of the samples are provided in Table 2.
 168 After addition of reagents to CBPD, the samples were homogenised with a mortar and a pestle
 169 and placed in cylindrical alumina crucibles in powder form. The samples were then placed in
 170 a muffle furnace preheated at 1100°C (for belite and mayenite) and 1200°C (for alite) to
 171 thermally treat in air for 30, 60, and 120 minutes. The samples, directly removed from the
 172 furnace still at the clinkering temperature and allowed to cool in air, were then ground with
 173 a mortar and a pestle.

174 *Table 2: Heating temperatures and amounts of SiO₂ and Al₂O₃ added to CBPD to produce specific clinker phases. All three*
 175 *sets were each heated for 30, 60, and 120 mins.*

Sample name	Target phase	Heating temperature (°C)	CBPD (g)	SiO₂ (g)	Al₂O₃ (g)
C₃S	Alite	1200	2.87	0.13	-
C₂S	Belite	1100	2.61	0.39	-
C₁₂A₇	Mayenite	1100	1.91	-	1.09

Cement phases are annotated using cement oxide notation: C = CaO, S = SiO₂, A = Al₂O₃.

176 **3.6. Behaviour of simplified CBPD**

177 In order to further investigate the effect of KCl and other constituents in the CBPD separately,
 178 six “simplified CBPD” compositions (S-CBPD 1 – 6) were prepared using CaCO₃ and SiO₂
 179 (stoichiometric to produce alite) with another constituent. The constituents considered are
 180 those with a significant composition (> 1 wt.%) in CBPD and the batch compositions of S-CBPD
 181 1 – 6 are provided in Table 3. The weight percentage of elements was based on their
 182 composition in the as-received CBPD. Calcium carbonate was generally used as a source of
 183 CaO, but its amount was slightly reduced when calcium sulfate dihydrate was used as a source
 184 of SO₃, since it will also provide CaO. The required chemicals were mixed and homogenised
 185 through grinding/mixing with a mortar and pestle for 10 minutes and placed into cylindrical
 186 alumina crucibles. The prepared samples were introduced into a muffle furnace preheated at

187 1200°C to thermally treat in air for 30 minutes. The heated samples were directly taken out
 188 from the furnace still at target temperature and ground with a mortar and pestle after cooling
 189 in air.

190

Table 3: Quantities of chemicals used in the simulated CBPD samples.

Sample	CaCO ₃ (g)	SiO ₂ (g)	Constituent of interest (g)
S-CBPD 1	2.59	0.41	-
S-CBPD 2	2.24	0.35	KCl (0.41)
S-CBPD 3	2.51	0.39	Al ₂ O ₃ (0.10)
S-CBPD 4	2.54	0.40	Fe ₂ O ₃ (0.06)
S-CBPD 5	2.52	0.40	MgO (0.08)
S-CBPD 6	2.44	0.41	Ca ₂ SO ₄ .2H ₂ O (0.15)

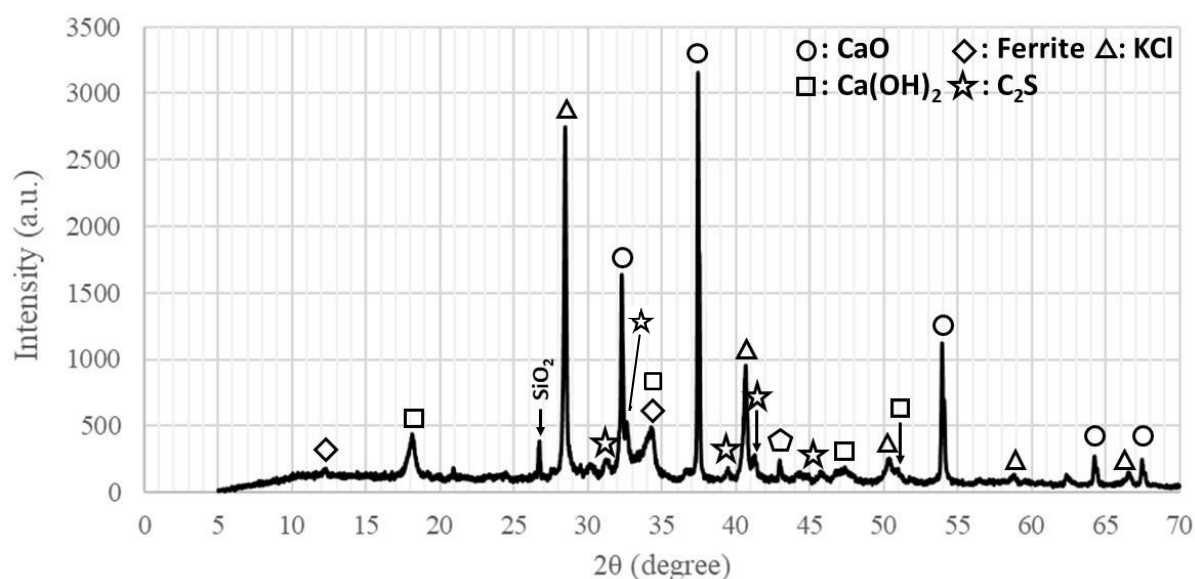
191

4. Results and Discussion

192

4.1. Characteristics of CBPD

193 The XRD results of CBPD reveals it is composed of CaO, KCl, SiO₂, and Ca(OH)₂ as major phases;
 194 the presence of belite and ferrite is also detected. The annotated XRD diffractogram of the
 195 raw CBPD is provided in Fig. 1. Table 4 shows the elemental composition of the CBPD obtained
 196 through XRF and ICP-OES analyses where constituents less than 0.1 wt.% are not included;
 197 two methods were used because sample preparation for XRF required processing at high
 198 temperatures, which could raise doubts due to the potential of KCl volatilization. The XRF and
 199 ICP analyses are in good agreement. If all Ca exists as oxide, more than 50 wt.% of CBPD is
 200 composed of CaO. If all the chlorine found in the XRF analysis is assumed to be bound to
 201 potassium as KCl as observed in the XRD data, this corresponds to 12.1 wt.% of KCl in the
 202 CBPD.



203

204

Figure 1: X-ray diffraction pattern of the raw cement kiln bypass dust (CBPD).

205

Table 4: Elemental composition (weight %) of cement kiln bypass dust obtained through both XRF and ICP-OES.

	Ca	Si	Cl	Al	K	Mg	S	Fe	Na	Br	I	Pb	Ti
XRF	38.0	6.9	5.8	2.1	9.4	1.7	0.9	1.6	0.4	0.5	0.3	0.16	0.1
ICP	35.8	6.7	-	1.4	8.6	1.5	0.9	1.5	0.4	-	-	0.13	0.1

Constituents less than 0.1 wt.% are not included

The ICP data for Si is from the samples dissolved in aqua regia/HF

The ICP data for Al, Fe, and Ti are taken from samples dissolved in HNO₃/HF

The ICP data for remaining elements are from samples dissolved in HNO₃ alone

206 A series of endothermic reactions are observed when CBPD is subjected to heating up to

207 1400°C as shown in the DSC data in Fig. 2; most of these events are associated with a weight

208 loss as observed in the TG data in Fig. 3. The weight loss at ~390°C can be attributed to the

209 decomposition of Ca(OH)₂ identified in XRD. The DSC peak at 573°C can be attributed to the

210 inversion of α-quartz to β-quartz. The weight loss over 500 – 1000°C may be attributed to the

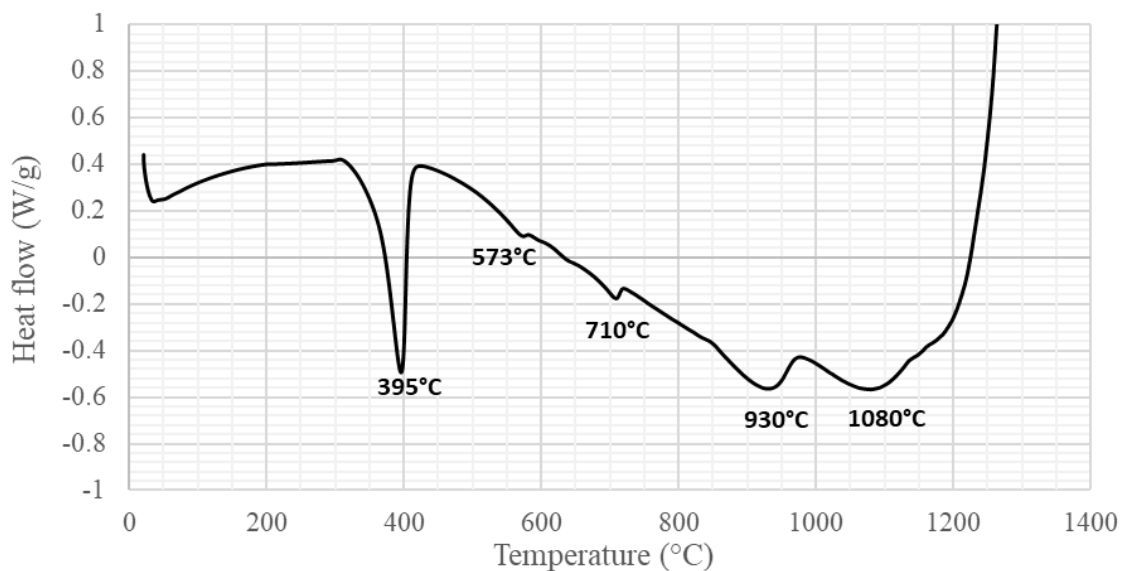
211 possible melting and subsequent vaporisation of alkali and/or alkaline earth salts. For

212 instance, the melting temperature of KCl is 770°C [18], and thus KCl can evaporate in this

213 temperature range. The amount of KCl estimated by XRF was 12.1 wt.%, which seems to form

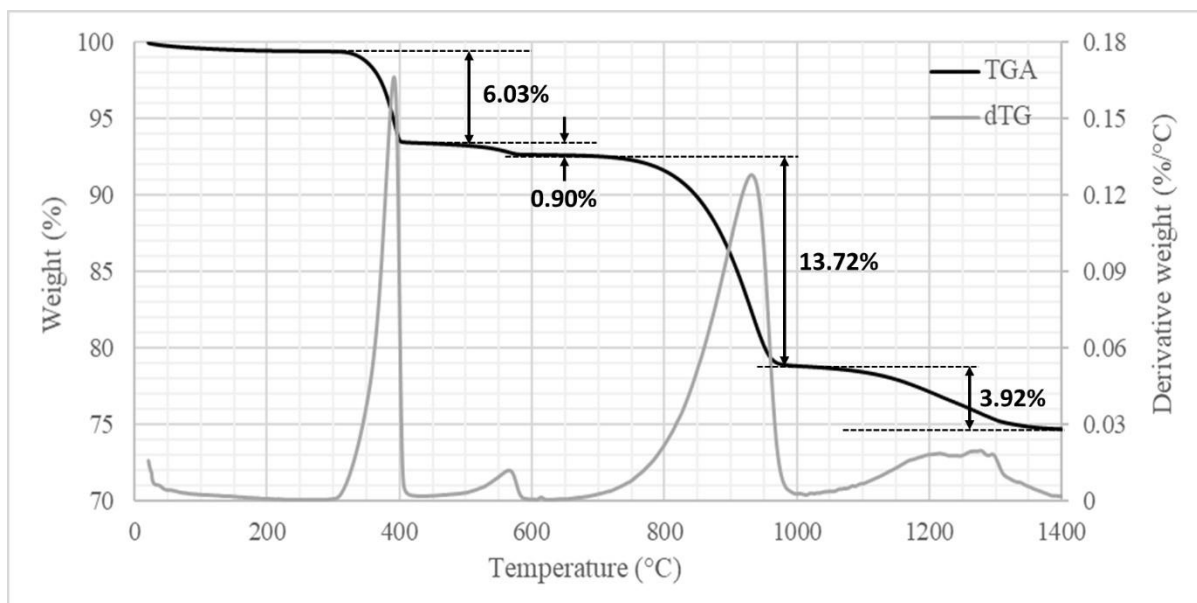
214 the majority of the weight loss observed in this temperature region in the TG data. The weight

215 loss above 1000°C is likely the evaporation of sulfate salts (e.g. K_2SO_4 or $MgSO_4$) as a significant
 216 amount of sulfur was identified in the XRF data.



217
 218

Figure 2: Differential scanning calorimetry analysis of cement kiln bypass dust.



219

220

Figure 3: TGA (black) and differential thermogravimetric (DTG) (grey) analysis of CBPD.

221

222 **4.2. Pyro processing CBPD: results**

223 Table 5 summarises the phase composition of the heated samples determined from
 224 qualitative XRD analyses; the table lists the cementitious clinker phases formed in the
 225 samples and also indicates the presence/persistence of KCl.

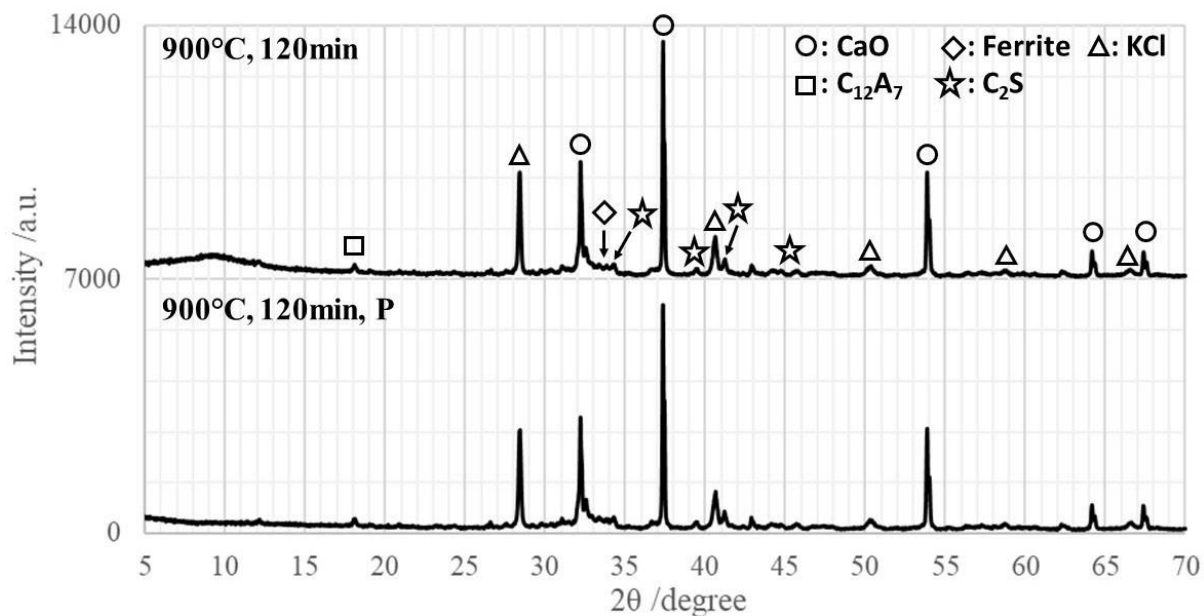
226 *Table 5: Cementitious phases produced in samples prepared for the title study. The presence of KCl is also shown.*
 227 *X denotes that the compound is not present while a circle (●) denotes that the compound is present. The sample*
 228 *ID indicates the temperature at which the samples were thermally treated except for the S-CBPD samples where*
 229 *all samples were heated to 1200 °C. The label "P" in the sample names indicates the pelletised samples. The*
 230 *detailed Al/Fe ratio was not determined for ferrite phases in the present work.*

Sample ID	Heating time (min)	C ₃ S	C ₂ S	C ₁₂ A ₇	C ₂ (A _x F _{1-x})	CA	CA ₂	KCl	
Raw CBPD	-	X	●	X	●	X	X	●	
CBPD_900	120	X	●	●	●	X	X	●	
CBPD_900_P									
CBPD_1100	30							●	
CBPD_1100_P									
CBPD_1100	60	X	●	●	●	X	X		
CBPD_1100_P									
CBPD_1100	120							X	
CBPD_1100_P									
CBPD_1200	30								
CBPD_1200_P									
CBPD_1200	60	●	●	●	●	X	X	X	
CBPD_1200_P									
CBPD_1200	120								
CBPD_1200_P									
C ₃ S_1200	30								
C ₃ S_1200	60	●	●	●	●	X	X	X	
C ₃ S_1200	120								
C ₂ S_1100	30							●	
C ₂ S_1100	60	X	●	●	●	X	X		
C ₂ S_1100	120							X	
C ₁₂ A ₇ _1100	30							●	
C ₁₂ A ₇ _1100	60	X	●	●	X	●	●	X	
C ₁₂ A ₇ _1100	120								
S-CBPD 1 (-)	30	X	●	X	X	X	X		
S-CBPD 2 (KCl)									
S-CBPD 3 (Al ₂ O ₃)			X	●	●	X	X	X	X
S-CBPD 4 (Fe ₂ O ₃)			X	●	X	●	X	X	
S-CBPD 5 (MgO)									
S-CBPD 6 (Ca ₂ SO ₄ .2H ₂ O)			X	●	X	X	X	X	

231 XRD patterns of the CBPD heated at 900°C, 1100°C, and 1200°C are shown in Figs. 4, 5, and 6
232 respectively. It should be noted that in the annotated XRD Figures, the ferrite assemblages:
233 $C_2(A_xF_{1-x})$ where $0 < x < 1$, are undifferentiated. The CBPD heated at 900°C (Fig. 3), in both
234 powder and pellet forms, showed similar patterns suggesting no significant advantage
235 through pellet pressing. $Ca(OH)_2$ present in the original CBPD was not observed in the sample
236 heated at 900°C, suggesting that $Ca(OH)_2$ has dehydroxylated. Mayenite, $C_{12}A_7$, a major phase
237 in calcium aluminate cement clinker, is present, and silica has reacted to form belite C_2S (no
238 SiO_2 is observed in Fig 4). However, KCl which is unwanted in the final clinker remains after
239 two hours of heating even though the peak intensity appears to be lower compared with the
240 original CBPD. Chloride is known to substitute into the mayenite structure; however, it is not
241 clear whether any Cl has incorporated into the mayenite.

242 The CBPD heated to 1100°C (Fig. 5) showed the presence of belite and mayenite. The KCl
243 content appears to decrease with heating time and is no longer observed after 120 minutes
244 of heating. Similarly, as shown in Fig. 6, upon heating to 1200°C, the peaks of KCl are not
245 discerned even after only 30 minutes of heating. This can be explained by the difference in
246 the vapour pressure of KCl at the different temperatures; vapour pressure data is provided in
247 Fig. 7. The vapour pressures of KCl at 1100°C and 1200°C are significantly higher than that at
248 900°C, and thus, KCl can evaporate easier at these higher temperatures.

249

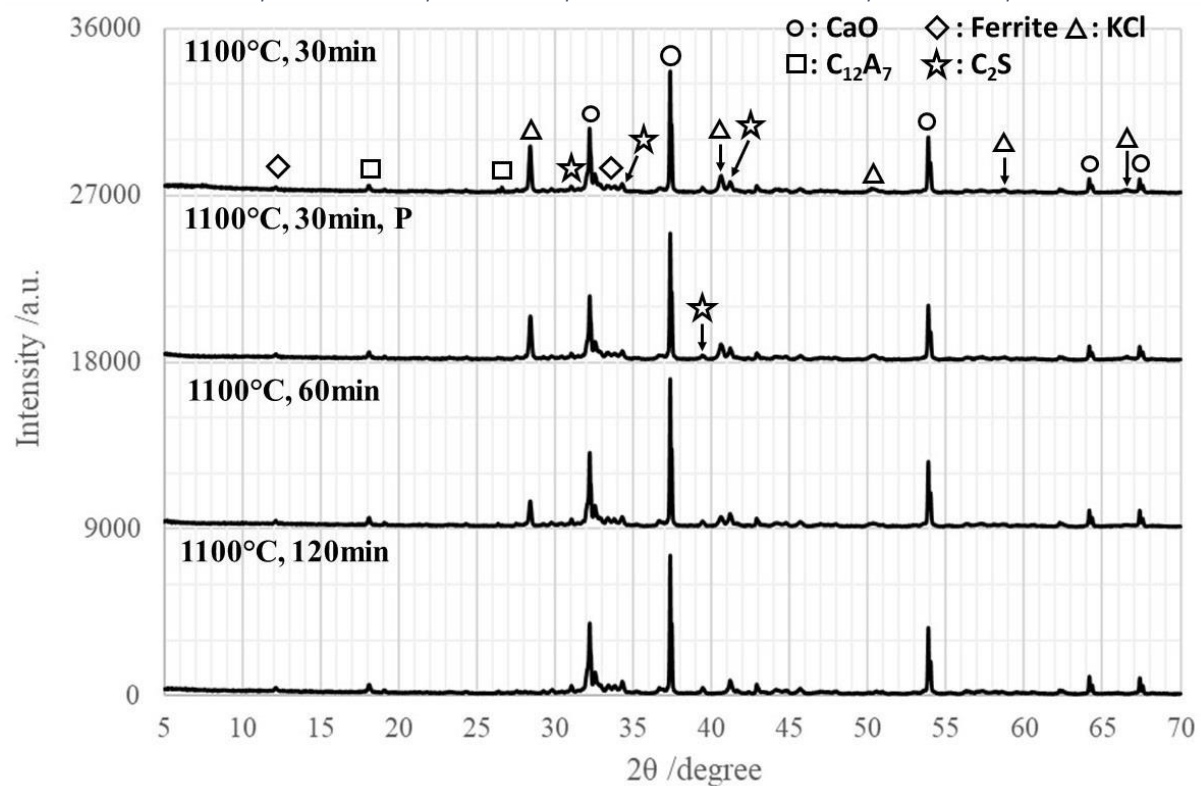


250

251

252

Figure 4: X-ray diffraction patterns of the cement kiln bypass dust heated at 900°C for 120 min showing the difference between pelletised and un-pelletized samples. The label "P" denotes the pelletised sample.



253

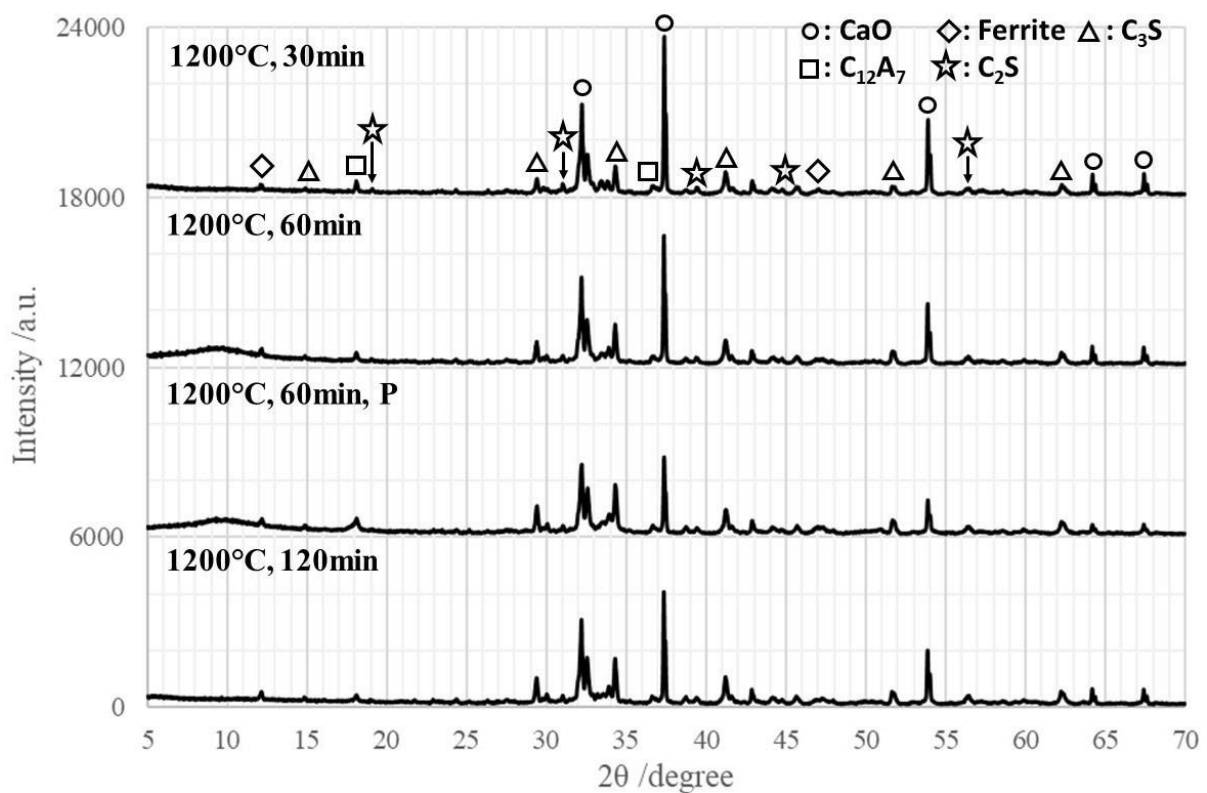
254

255

256

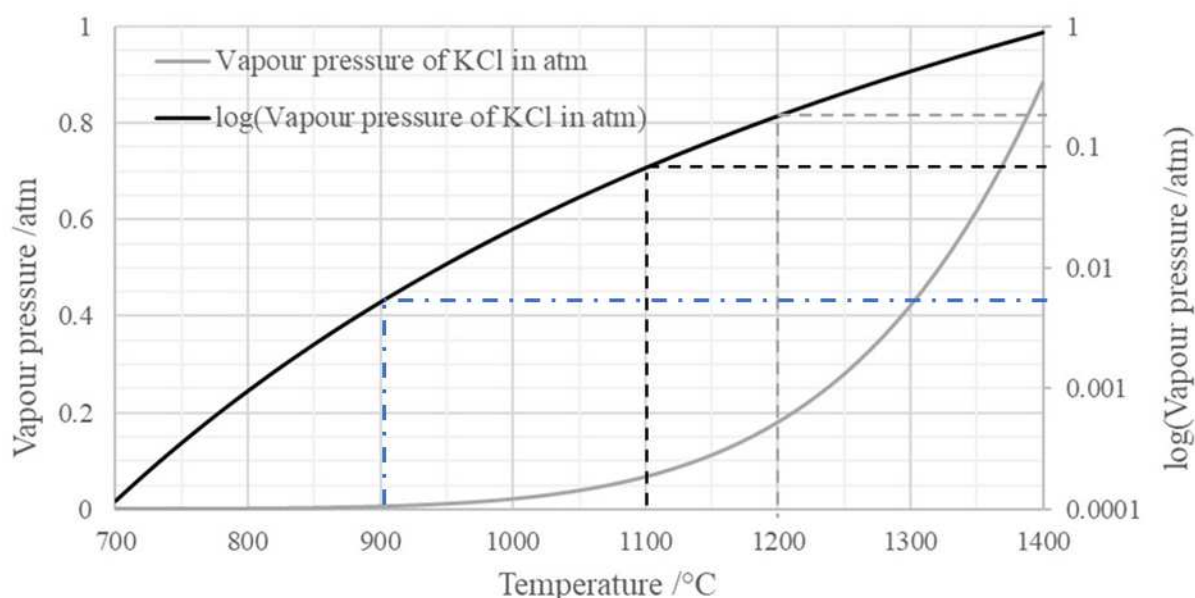
Figure 5: X-ray diffraction patterns of the cement kiln bypass dust heated at 1100°C for 30, 60, and 120 min. The label "P" denotes the pelletised sample.

257 Unexpectedly, all the samples heated to 1200°C showed the formation of alite which is
 258 normally produced industrially at temperatures greater than 1400°C and thermodynamically
 259 unstable below 1250°C [19]; pure alite is usually formed in-lab at higher temperatures of
 260 1600°C [20]. This is a significantly lower temperature than normally used in the cement
 261 industry for alite formation. Components in the CBPD contributed to lowering the formation
 262 temperature of alite and enhancing its formation; however, the exact mechanism is still not
 263 apparent.



264

265 Figure 6: X-ray diffraction patterns of the CBPD samples heated at 1200 °C for 30, 60, and 120 min. The sample labelled "P"
 266 denotes the pelletised sample.



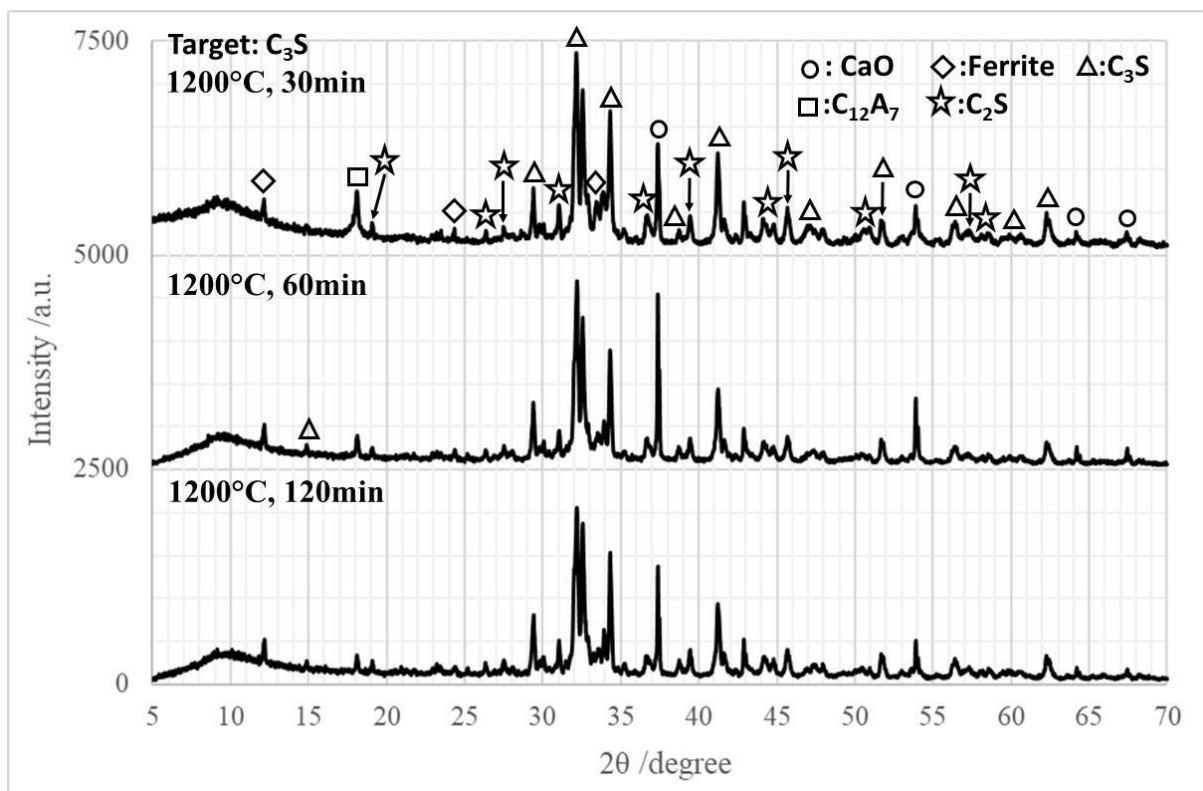
267
 268 *Figure 7: The vapour pressure of potassium chloride as a function of temperature. The left; primary axis shows a linear scale*
 269 *(grey line) while the right; secondary axis shows a logarithmic scale of the same data (black line). The data is taken from the*
 270 *Dortmund Data Bank for saturated vapor pressure calculations (available at:*
 271 *http://www.ddbst.com/en/EED/PCP/VAP_C4577.php).*

272 It was noted that the weight of samples decreased by approximately 20% on average after
 273 heating at 1200°C, which agrees well with the thermogravimetric analyses shown in Fig. 3.
 274 There was no significant difference between samples in powder and pellet forms in the range
 275 of heating temperatures and heating durations tested; hence, only powder samples were
 276 produced in further experiments.

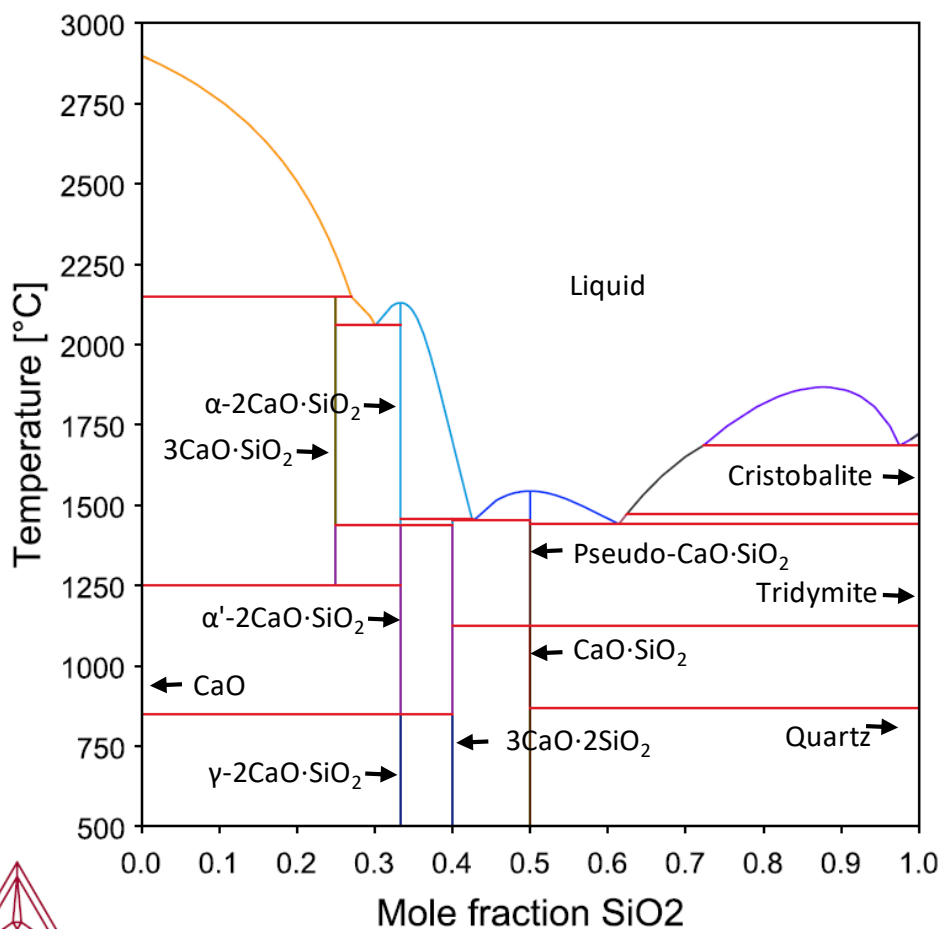
277 **4.3. Interaction of CBPD with additives: results**

278 Figure 8 shows the XRD patterns of the CBPD samples with additional silica targeted to
 279 produce alite at 1200°C. As shown in the figure, when additional silica was introduced, the
 280 peaks for alite and belite clearly became more intense compared with the previous CBPD
 281 samples heated at 1200°C without any additions (Fig. 6). However, it is apparent that
 282 significant quantities of free CaO are present and did not completely react with belite to form

283 alite. This may suggest the limited reaction between CaO and belite in the conditions tested.
 284 As observed in the CaO-SiO₂ phase diagram presented in Fig. 9, C₃S formed at high
 285 temperatures can decompose into CaO and C₂S at lower temperatures; however, due to the
 286 low quantities of material processed and the temperature of the ambient (~20°C), the
 287 produced clinker can be assumed to have been quenched; thus, decomposition of alite during
 288 the cooling of the samples would not have occurred. Either way, the tested conditions
 289 designed to utilise all Ca component of CBPD for the formation of alite was insufficient for the
 290 complete conversion to alite at 1200°C, but sufficient to manufacture a clinker that contains
 291 alite as a major phase.



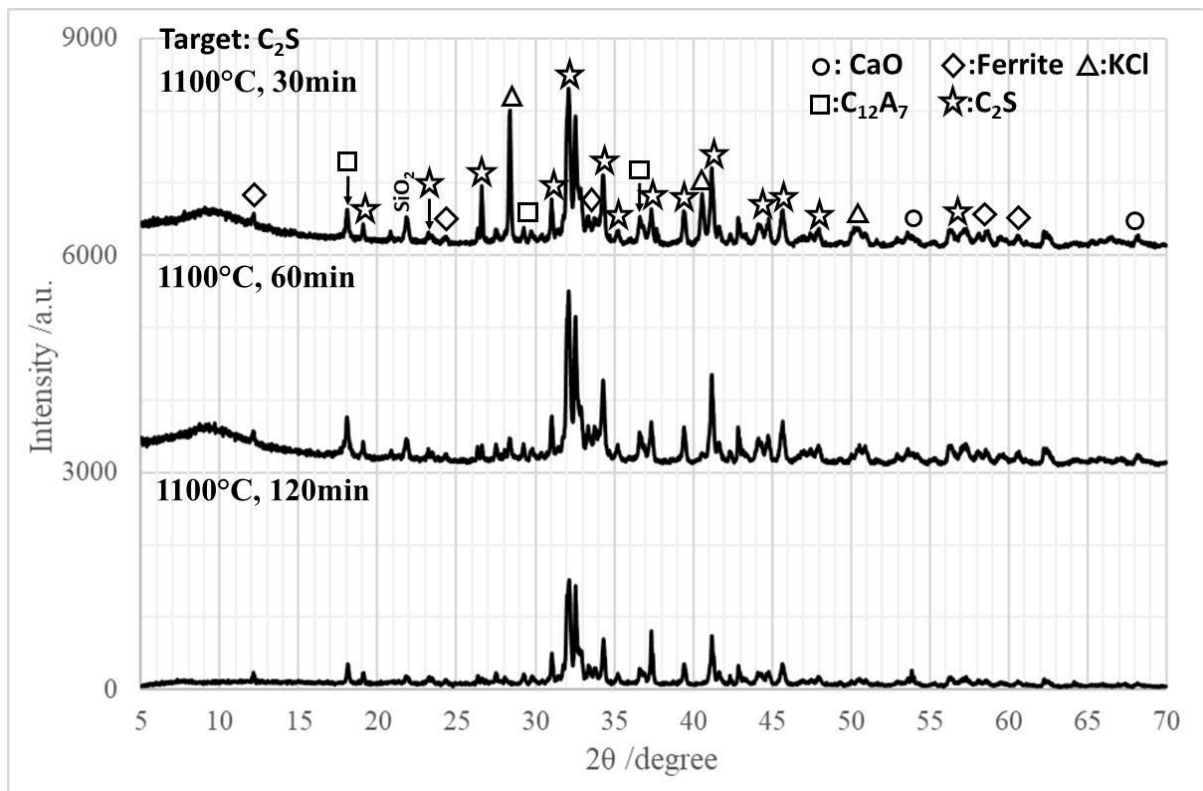
292 Figure 8: XRD patterns of the cement kiln bypass dust samples mixed with silica for creating alite at 1200 °C while heating
 293 for 30, 60, and 120 minutes.
 294



295

296 *Figure 9: CaO-SiO₂ phase diagram was calculated using Thermo-Calc Software [21] with Thermo-Calc Software OXDEMO:*
 297 *Oxide demo database v2.0*

298 XRD patterns of the CBPD samples with additional silica targeted to produce belite (C₂S) at
 299 1100°C are provided in Fig. 10. A significant increase in intensity is observed for the peaks of
 300 belite when compared with the CBPD samples heated without any additions. The XRD
 301 patterns also showed the presence of SiO₂ (cristobalite) at ~22° 2θ which is a high
 302 temperature polymorph of unreacted SiO₂, which decreases when reaction time is extended
 303 to 120 minutes. The presence of any unreacted SiO₂ may be attributed to some of the CaO in
 304 CBPD being combined as mayenite and ferrite, which were not targeted.

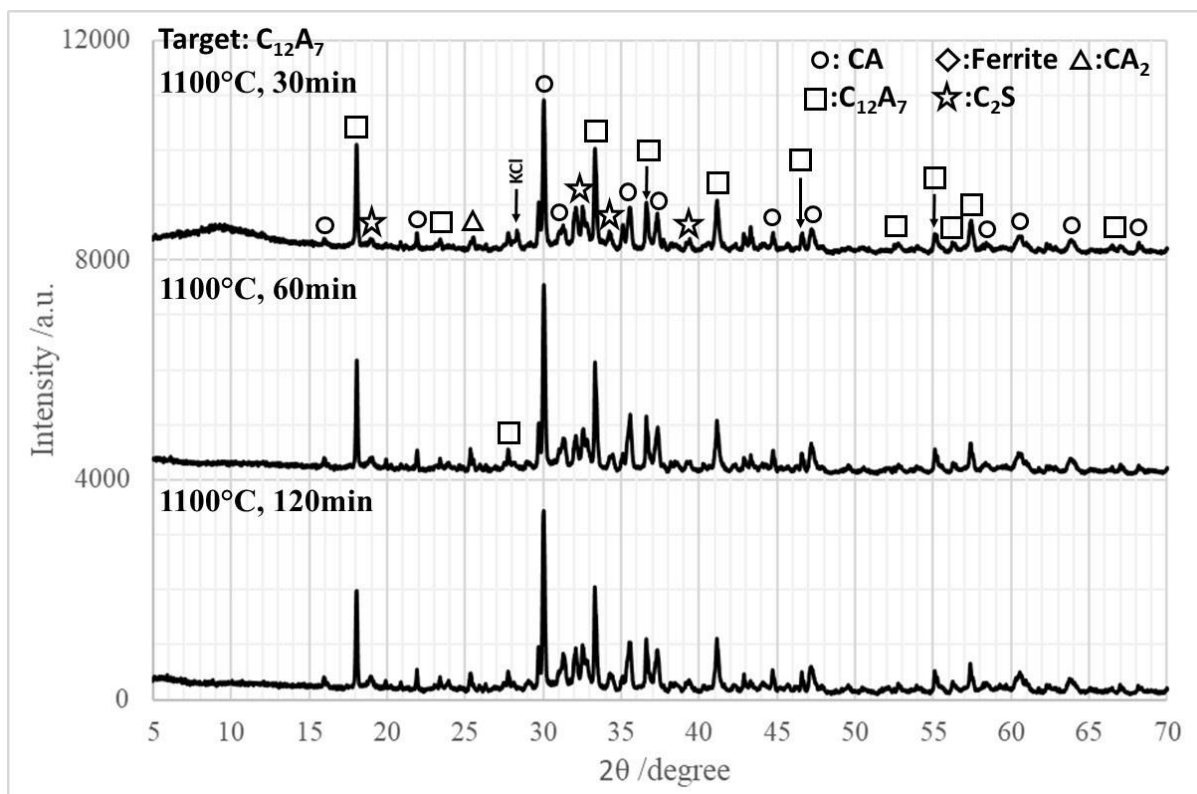


305
306

Figure 10: XRD patterns of samples mixed with silica for creating belite at 1100 °C while heating for 30, 60, and 120min.

307 The XRD patterns of the samples with additional alumina targeted to produce mayenite
 308 ($C_{12}A_7$) at 1100°C are also provided in Fig. 11. A clear increase in mayenite content was
 309 observed when compared with the CBPD samples heated at 1100°C without any additions.
 310 This system also produced a significant amount of mono-calcium aluminate (CA) and trace
 311 amount of CA_2 . CA is a known cementitious phase whereas CA_2 is weakly hydraulic [22]. The
 312 production of CA and CA_2 can be attributed to some of the CaO in CBPD being combined as
 313 belite and ferrite. The reactions of CBPD at 1100°C targeting belite or mayenite suggest that
 314 the production of belite and mayenite from CBPD can be increased by adding silica or alumina
 315 and that there was minimal unreacted SiO_2 or Al_2O_3 after 120 minutes. They also had minimal
 316 to no free lime (CaO). The interaction of CBPD with additional silica or alumina resulted in the

317 formation of both targeted and untargeted hydraulic phases; this shows that the CBPD is
 318 favourable for the formation of various cementitious clinker phases and phase assemblages.



319
 320 *Figure 11: XRD patterns of samples mixed with alumina for creating mayenite at 1100 °C while heating for 30, 60, and 120*
 321 *minutes.*

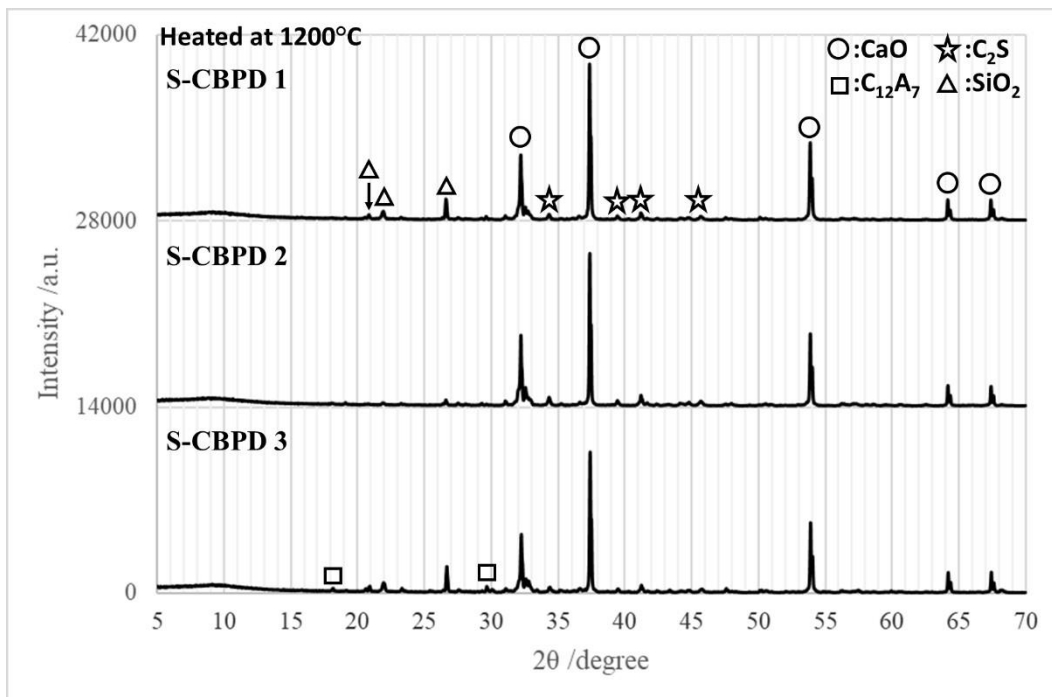
322 It should be noted that there was a gradual decrease in the intensity of KCl peaks in the
 323 samples heated at 1100°C, while no peaks of KCl were observed when heated at of 1200°C
 324 even as short as 30 min; consistent with that found in CBPD samples without additives. This
 325 loss of KCl at early stage (within 30 min) could be potentially one of the reasons for the limited
 326 combination of CaO at 1200°C. As previously mentioned, such salts can act as a flux to
 327 improve the extent of reactions [14]. Further study is necessary to elucidate this point.

328

329 4.4. Behaviour of simplified CBPD: results

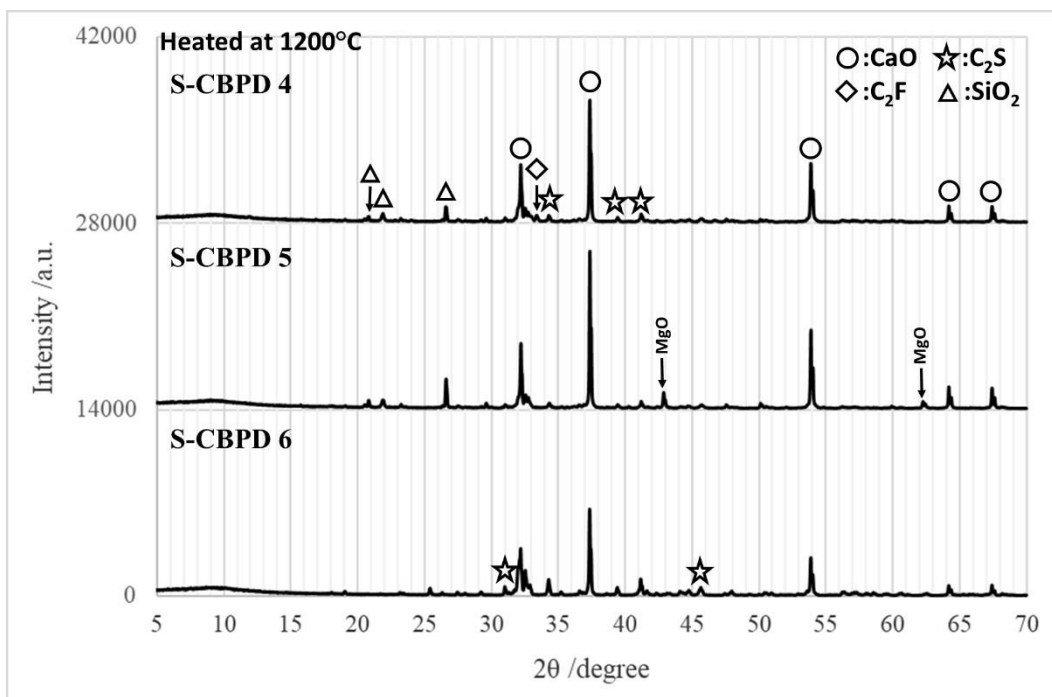
330 One of the key findings in the previous sections was the formation of alite from CBPD at
331 1200°C both with and without additional silica added. The effects of major constituents in
332 CBPD on the reactivity of the system were studied by making “simplified CBPD” composed of
333 CaCO₃ and SiO₂ alone and with one other constituent shown in the elemental analyses of raw
334 CBPD namely: KCl, Al₂O₃, Fe₂O₃, MgO, and CaSO₄.2H₂O.

335 The diffraction patterns for the “simplified CBPD” samples are shown in Figs. 12 and 13. The
336 significant reduction of the peak intensity of SiO₂ in S-CBPD 2 confirms that KCl does indeed
337 enhance the formation of belite. The sample with added gypsum also showed lower intensity
338 peaks for silica, suggesting the enhanced reaction of silica. The peak intensity for CaO also
339 appears to be lower in the system with added gypsum. However, no other calcium silicate
340 reaction products were identified. In addition to belite, the formation of mayenite was
341 observed through adding Al₂O₃ while dicalcium ferrite (C₂F) was formed with the addition of
342 Fe₂O₃. The presence of MgO appears to have a limited participation in the reaction of the
343 system.



344

345 Figure 12: X-ray diffraction patterns of the "simplified" CBPD samples prepared from CaCO₃, SiO₂, and a third additive: 1 =
346 no additive; 2 = KCl; 3 = Al₂O₃.



347

348 Figure 13: X-ray diffraction patterns of the "simplified" CBPD samples prepared from CaCO₃, SiO₂, and a third additive: 4 =
349 Fe₂O₃; 5 = MgO; 6 = CaSO₄·2H₂O.

350

351 None of the S-CBPD samples produced alite; therefore, it can be inferred that the formation
352 of alite by pyro processing CBPD at 1200°C with and without addition of silica is due to a
353 synergetic effect between the constituents, for example, that the presence of S and Cl may
354 have allowed for the formation of chlorellestadite ($\text{Ca}_{10}(\text{SiO}_4)_3(\text{SO}_4)_3\text{Cl}_2$) which may enhance
355 alite formation [23]; however, no chlorellestadite was detected through XRD. The presence
356 of iron in the clinker raw-mixes has also been found to aid alite formation at lower
357 temperatures in the presence of a flux [24], and this may have also been a contributing
358 component.

359 **5. Further discussion**

360 The present work shows that CBPD can be thermally treated to produce clinker phases at
361 lower temperatures than is conventional. Real life applications can involve pyro processing
362 CBPD with other raw materials such as aluminosilicate clays to produce modified cement
363 clinker or even supplementary cementitious material free from uncombined CaO. However,
364 this may not be directly applicable in existing kiln configurations due to the volatilisation of
365 salts which were an initial reason for the bypass dust being withdrawn/generated.
366 Nonetheless, another calcination process, not utilizing the traditional counter-current kiln can
367 be employed for the pyro processing of raw material feed containing significant amounts of
368 CBPD. For example, the new process can be a batch reactor with a salt separation/deposition
369 system. The collected salt can then be used as commodity or in another process or recycled
370 for the manufacture of cementitious materials using other calcareous and aluminosilicate raw
371 materials. Additionally, due to the lower temperatures required for clinker phase

372 manufacture in the presence of the salt/KCl, it may be possible to use indirect or electrically
373 heated furnaces; which, if powered from sustainable/green sources, will result in the
374 production of a zero-carbon cementitious material as their will be minimal associated
375 chemical and process carbon emissions. Lower formation temperatures can also enable the
376 utilisation of lower quality alternative fuels such as biomass; nonetheless, further work is
377 required to optimise clinker or SCM production and formulations from CBPD and design of a
378 new calcination process/unit.

379 The composition of CBPD will vary by location of the plants due to changes minor constituents
380 of fuels and local raw materials, as well as plant configurations where CBPD may be combined
381 with CKD; however, these variations can be managed through blending with additives during
382 raw-mix design of material to be processed. While the industrial pyro processing of CBPD will
383 most probably require capital investment in any cement plant, this could be cost competitive
384 since the costs of transport and landfill are generally high.

385 The valorisation of CBPD for clinker manufacture will also contribute to reduce the cost of CO₂
386 emission, as the CBPD is a source of already decarbonised CaO, which is key for clinker
387 manufacture. The reduced formation temperature of clinker phases can also translate to a
388 reduction energy demand and in fuel-derived CO₂ emissions when compared to the
389 conventional Portland cement manufacturing process. Additionally, unlike limestone rock,
390 the CBPD will not require grinding prior to pyro processing.

391 The properties of hardened cement made from clinker produced through the pyro processing
392 of CBPD still needs to be assessed in terms of its chemical, rheological, mechanical, and

393 durability performance. The work here has shown that the Cl-containing salt(s) can be driven
394 off through the heating process, but the effects of any Cl remaining in the cement is still
395 unknown. Additionally, the effects of any potential substitution or persistence of alkali (e.g.,
396 potassium) in the clinker/cement and subsequent concrete material will need to be assessed.

397 In agreement with previous works [15, 16], the formation of belite and mayenite is observed
398 in this work at temperatures as low as 900°C in the presence of a molten-salt flux. However,
399 the final product still contained the salt after cooling from 900°C. Future works should also
400 attempt to produce cement phases at such low temperatures while optimising the amount of
401 salt in the mix before and after thermal treatment; other molten salts can also be tested.
402 Previous studies [25, 26] have also shown that the CBPD which contain large quantities of
403 undesired constituents, such as chlorides, may be classified or separated mechanically to
404 reduce the quantities of these undesired constituents to required limits.

405 **6. Conclusions**

406 Cement kiln bypass dust can be valorised through thermal treatment for the manufacture of
407 cement clinker or supplementary cementitious materials. The formation of cement clinker
408 phases such as belite, mayenite, alite, and ferrite is enhanced by the minor components
409 intrinsic to CBPD, in particular KCl. Clinker Phase formation temperatures can be reduced, and
410 reaction kinetics can be improved when compared to the utilisation of the conventional raw
411 materials. Silica and alumina containing raw materials can be mixed with the CBPD, before
412 firing, to produce complete cement clinker phase assemblages and free of uncombined CaO.

413 The formation of alite at 1200°C is a significant observation of this work. It suggests that CBPD
414 can potentially be used to produce alite based cements (e.g. Portland cement) at lower
415 temperatures than that of the conventional process. The exact mechanism for the low
416 temperature alite formation observed through the thermal treatment of CBPD requires
417 further investigation but it is apparent that the intrinsic chloride salt plays a vital role.

418 By heating at temperatures as low as 1100°C, the salt is removed/evaporated from the system
419 leaving behind a cementitious product free from majority of the undesired alkali chlorides
420 and other undesired salts which are initially present. The produced clinker phases have a
421 lower production temperature and thus can have lower fuel-derived CO₂ emissions.
422 Additionally, the CaO in CBPD exists in an already decarbonised form; therefore, the clinker
423 produced from CBPD has a lower raw-material CO₂ footprint than conventional cement
424 clinker produced from the virgin raw materials. Outcomes of this work also encourage
425 attention to the use of chloride salts as a flux for cement clinker manufacturing.

426 **Acknowledgements**

427 This research was partially funded by the Engineering and Physical Science Research Council
428 (EPSRC) through grant: EP/R025959/1. This work was performed in part at the MIDAS facility
429 at the University of Sheffield which was established with support from the department of
430 energy and climate change. The authors would like to acknowledge the support of Olga
431 Chowaniec who facilitated this work and thank Heather Grievson for conducting the ICP-OES
432 analyses.

433 **References**

- 434 1. Olivier, J.G.J., et al., *Trends in global CO2 emissions: 2016 Report*. 2016, PBL Netherlands
 435 Environmental Assessment Agency Hague and European Commission Joint Research Centre
 436 Institute for Environment and Sustainability.
- 437 2. Zhang, C.-Y., et al., *Accounting process-related CO2 emissions from global cement production*
 438 *under Shared Socioeconomic Pathways*. Journal of cleaner production, 2018. **184**: p. 451-465.
- 439 3. Oss, H.G.v., *U.S. Geological Survey, Mineral Commodity Summaries:Cement*. 2019, National
 440 Minerals Information Center.
- 441 4. Darley, E.F., *Studies on the effect of cement-kiln dust on vegetation*. Journal of the air pollution
 442 control association, 1966. **16**(3): p. 145-150.
- 443 5. Bertoldi, M., et al., *Health effects for the population living near a cement plant: An*
 444 *epidemiological assessment*. Environment international, 2012. **41**: p. 1-7.
- 445 6. Nocuń-Wczelik, W. and K. Stolarska, *Calorimetry in the studies of by-pass cement kiln dust as*
 446 *an additive to the calcium aluminate cement*. Journal of Thermal Analysis and Calorimetry,
 447 2019. **138**(6): p. 4561-4569.
- 448 7. Ata, A.A., T.N. Salem, and N.M. Elkhawas, *Properties of soil–bentonite–cement bypass mixture*
 449 *for cutoff walls*. Construction and Building Materials, 2015. **93**: p. 950-956.
- 450 8. Ghorab, H.Y., A. Anter, and H. El Miniawy, *Building with local materials: stabilized soil and*
 451 *industrial wastes*. Materials and manufacturing processes, 2007. **22**(2): p. 157-162.
- 452 9. Al-Aghbari, M.Y., Y.-A. Mohamedzein, and R. Taha, *Stabilisation of desert sands using cement*
 453 *and cement dust*. Proceedings of the Institution of Civil Engineers-Ground Improvement, 2009.
 454 **162**(3): p. 145-151.
- 455 10. Al-Jabri, K.S., et al., *Effect of copper slag and cement by-pass dust addition on mechanical*
 456 *properties of concrete*. Construction and building materials, 2006. **20**(5): p. 322-331.
- 457 11. El Sherbiny, S.A., et al., *Use of cement dust in the manufacture of vitrified sewer pipes*. Waste
 458 management, 2004. **24**(6): p. 597-602.
- 459 12. Khater, G.A., *Use of bypass cement dust for production of glass ceramic materials*. Advances
 460 in applied ceramics, 2006. **105**(2): p. 107-111.
- 461 13. Abdel-Gawwad, H.A., et al., *Sustainable disposal of cement kiln dust in the production of*
 462 *cementitious materials*. Journal of Cleaner Production, 2019. **232**: p. 1218-1229.
- 463 14. Liu, X., N. Fechler, and M. Antonietti, *Salt melt synthesis of ceramics, semiconductors and*
 464 *carbon nanostructures*. Chemical Society Reviews, 2013. **42**(21): p. 8237-8265.
- 465 15. Hanein, T., et al., *Prospects for manufacturing cement compounds in molten salt fluxed*
 466 *systems*, in *37th Cement and Concrete Science Conference*. 2017: London, UK.
- 467 16. Hanein, T., et al. *Molten salt synthesis of compounds related to cement*. in *First International*
 468 *Conference on Cement and Concrete Technology*. 2017. Muscat, Oman.
- 469 17. Photiadis, G., et al., *Low energy synthesis of cement compounds in molten salt*. Advances in
 470 Applied Ceramics, 2011. **110**(3): p. 137-141.
- 471 18. Bale, C.W., et al., *Reprint of: FactSage thermochemical software and databases, 2010–2016*.
 472 Calphad, 2016. **55**: p. 1-19.
- 473 19. Hanein, T., F.P. Glasser, and M.N. Bannerman, *Thermodynamic data for cement clinkering*.
 474 Cement and Concrete Research, 2020. **132**(106043).
- 475 20. Wesselsky, A. and O.M. Jensen, *Synthesis of pure Portland cement phases*. Cement and
 476 concrete research, 2009. **39**(11): p. 973-980.

- 477 21. Andersson, J.-O., et al., *Thermo-Calc & DICTRA, computational tools for materials science.*
478 Calphad, 2002. **26**(2): p. 273-312.
- 479 22. Klaus, S.R., J. Neubauer, and F. Goetz-Neunhoeffler, *Hydration kinetics of CA2 and CA—*
480 *investigations performed on a synthetic calcium aluminate cement.* Cement and Concrete
481 Research, 2013. **43**: p. 62-69.
- 482 23. Chen, M. and Y. Fang, *The chemical composition and crystal parameters of calcium*
483 *chlorosulfatosilicate.* Cement and Concrete Research, 1989. **19**(2): p. 184-188.
- 484 24. Hanein, T., et al., *Alite calcium sulfoaluminate cement: chemistry and thermodynamics.*
485 Advances in Cement Research, 2019. **31**(3): p. 94-105.
- 486 25. Lanzerstorfer, C., *Residue from the chloride bypass de-dusting of cement kilns: Reduction of*
487 *the chloride content by air classification for improved utilisation.* Process Safety and
488 Environmental Protection, 2016. **104**: p. 444-450.
- 489 26. Sutou, K., H. Harada, and N. Ueno. *Chlorine bypass system for stable kiln operation and the*
490 *recycling of waste.* 1999. IEEE.

491